Exploring deuterium beam operation and the behavior of the co-extracted electron current in a negative-ion-based neutral beam injector

Exploring Deuterium Beam Operation and the Behavior of the Co-Extracted Electron Current in Negative-Ion-Based Neutral Beam Injector

K. Ikeda[1]**, K. Tsumori**[1,2]**, H. Nakano**[1,2]**, M. Kisaki**[1,2]**,**
K. Nagaoka[1,3]**, S. Kamio**[1]**, Y. Fujiwara**[1]**, Y. Haba**[3]**,**
and M. Osakabe[1,2]

[1] National Institute for Fusion Science (NIFS), Toki, 509-5292, Japan

[2] SOKENDAI (Graduate School for Advanced Studies), Toki 509-5292, Japan

[3] Graduate School of Engineering, Nagoya University, Nagoya 464-8603, Japan

E-mail: ikeda.katsunori@lhd.nifs.ac.jp

Abstract. Achievements of the deuterium beam operation of the negative-ion-based neutral beam injector (N-NBI) in the Large Helical Device (LHD) are reported. In the beam operation in LHD-NBIs, both hydrogen (H) and deuterium (D) neutral beams were generated by changing the operation gas using the same accelerator. The maximum accelerated deuterium negative ion current ($I_{acc(D)}$) reaches 46.2 A from two beam sources with the averaged current density being 190 A/m^2 for 2 sec, and the extracted electron to accelerated ion current ratio ($I_e/I_{acc(D)}$) increases to 0.39 using 5.6 V high bias voltage in the first deuterium operation in 2017. Increase of electron density in the vicinity of the plasma grid surface, which is considered the main reason of increasing co-extracted electrons in a beam, is confirmed by half-sized research negative ion source in the neutral beam test stand in NIFS. The deuterium negative ion density is also larger than the hydrogen negative ion density in the vicinity of plasma grid surface using the same discharge condition. In the latest experimental campaign in 2018, the $I_{acc(D)}$ increases to 55.4 A with the averaged current density being 233 A/m^2 for 1.5 sec using the shot extraction gap length. The low $I_e/I_{acc(D)}$ of 0.31 can be maintained by high discharge power. The various parameters mentioned above are defined in detail below.

Keywords: negative-ion, co-extracted electron, NBI

1. Introduction

Production of high intensity negative ion beams with low co-extracted electrons is a common issue for a negative-ion-based neutral beam injector (N-NBI) for heating and current drive in magnetically confined fusion device. Deuterium N-NBI with the beam energy of 500 keV in JT-60U [1,2] and hydrogen N-NBI with the beam energy of 180 keV in LHD [3–7] worked in Japan from 1996 and from 1998, respectively, with the latter reaching the full power specification for 2 sec beam in 2003 [8]. An N-NBI generating 1 MeV deuterium ions for 1 hour being developed for ITER [9,10], and the experiment of SPIDER [11,12] has started in 2018 in the ITER-NBI test facility in Padova. In the ITER-NBI, a deuterium beam of 40 A is planned with the beam energy of 1 MeV in the D-D and the D-T experiment phases, but the NBI will be operated at 870 keV and 46 A hydrogen beam in early hydrogen experiment phase [10]. Increase of co-extracted electrons for deuterium negative ion beam operation has been observed by the ITER half size source [13], which is an important issue for the realization of ITER-NBI. Therefore, optimization of generation negative ions and suppression of co-extracted electron current for both hydrogen and deuterium are required.

In the LHD, the first deuterium beam operation of the N-NBI was initiated in 2017 [14]. We generated both hydrogen and deuterium negative-ion beams in N-NBIs by changing the operation gas using the same accelerator. After the LHD experiment campaign, we investigated the characteristics of the negative ion density and the electron density by a research negative ion source (RNIS) in the neutral beam test stand (NBTS) in NIFS. Comparison of the beam properties such as the extracted negative ion current and the co-extracted electron current and source properties with H_2 and D_2 gases will clarify the production and extraction mechanism of the negative ions. This should contribute to the ITER and future NBIs.

This paper describes the results of hydrogen and deuterium beam operations in LHD-NBI. Changes in the negative ion current and electron current clearly appeared when the discharge gas was changed from hydrogen to deuterium. We will show the electron current and electron-ion current ratio, which clearly depends on the arc discharge power. We also show changes in the negative ion density and the electron density in the vicinity of cesiated metal surface in the negative ion source, and will discuss the similarity to the deuterium negative ion current and the electron current, respectively.

Various parameters mentioned in the abstract and in the following text are defined below. It is to be noted that the typical time of beam extraction was between 1.5 sec and 2 sec in high power beam operation in LHD-NBI. Only small variations ($< 5\%$) of the various parameters discussed below occurred over that period and the values quoted are averaged over the beam extraction period.

- Deuterium negative ion current ($I_{acc(D)}$):This is the electrical current to the grounded grid of the accelerator and the components downstream of the grounded grid when the ion source is operated with D_2 gas. That current will contain some

electrons created by stripping in the acceleration gap and some electrons escaping through the extraction grid into the acceleration gap. The fraction of electrons is estimated to be typically $\approx 13\%$.

- Hydrogen negative ion current($I_{acc(H)}$):This is the electrical current to the grounded grid of the accelerator and the components downstream of the grounded grid when the ion source is operated with H_2 gas. That current will contain some electrons created by stripping in the acceleration gap and some electrons escaping through the extraction grid into the acceleration gap. The fraction of electrons is estimated to be typically $\approx 10\%$.

- Electron current (I_e):This is the current to the extraction grid, which is defined $I_e = I_{ex} - I_{acc}$, here I_{ex} is the electrical current to the extraction grid. Electrons extracted from the ion source and electrons created by the stripping of extracted negative ions in the extraction gap and the aperture in the extraction grid are deflected onto the extraction grid by the magnetic field of the electron deflection magnets embedded in the grid. It was estimated that $\approx 97\%$ of those electrons are absorbed by the extraction grid, and that 3% escape into the acceleration gap [15]. The number of electrons created by stripping is typically $\approx 3\%$, so the current to the extraction grid is $\approx 106\%$ of the extracted electron current.

- Averaged negative ion current density:This is the deuterium or hydrogen negative ion current (defined as above) divided by the area of the apertures in the plasma grid.

- Filling pressure:The gas flow into the ion source is adjusted to give a chosen "filling pressure", which is the pressure in the ion source when the discharge is not operating (and there is no ion extraction). The gas flow is kept constant before and during source operation and ion extraction, but the gas pressure in the source will change significantly during source operation because the gas is heated by the discharge, there will be significant dissociation of the gas, and because ions are extracted from the source.

2. Ion Source Setting and Operation Conditions

2.1. Deuterium operation in LHD-NBI

The first deuterium experiment of the LHD was initiated after reference plasma discharge using hydrogen. Two positive-ion-based NBIs (P-NBI) and three N-NBIs are equipped in the LHD [16]. Before the deuterium experiment, the beam energy of P-NBI was upgraded from 40 keV to 60 keV and to 80 keV in the beam line four (BL4) and the beam line five (BL5), respectively, to concentrate the deuterium beam operation. The beamlet focusing condition is also optimized for deuterium by wide gap distance [17]. The nominal injection power increased from 6 MW to 9 MW in each beam line, which are contributed to increase ion temperature in deuterium discharges.

On the other hand, the beam energies in three N-NBIs are not increased to suppress neutron generation by D-D reaction of beam component within permissible neutron budget (2.1×10^{19}/year [18,19]) in LHD. Two hydrogen negative ion sources are equipped in one beam line [20]. The nominal beam energy is 180 keV in three beam lines, and an acceleration voltage is applied between an extraction grid (EG) and a grounded grid (GG), which is 70 mm for the first beam line (BL1) and 60 mm for the second beam line (BL2) and the third beam line (BL3) optimized for hydrogen operation. For this reason, the maximum injection power can be obtained by hydrogen beam operation. Therefore, the highest ion temperature was achieved using a hydrogen beam from N-NBIs and a deuterium beam from P-NBI in LHD deuterium experiment campaign. We uses a slot type GG [6, 21] in BL1 and BL3. The GG is equipped with the 55 slots, and is divided into five segments. The slot width is 14 mm with the transparency of 76 % in BL3, which is much higher than the transparency of 50 % for a conventional aperture type of GG (diameter of the aperture = 16 mm and 770 apertures in one source) in BL2. Improvement in transparency reduces the thermal load on the GG due to the peripheral components of negative ion beam, and reduces the number of electrical breakdowns in the accelerator. However, since the focusing conditions of the slit type GG are different in the vertical direction and the horizontal direction, the aperture shape of the steering grid on the back surface of the EG is arranged to the racetrack shape [22] to adjust beam divergence. The extraction gap length between a plasma grid (PG) and an the EG is also an important setting in a perveance condition of an ion beam. In the BL3, the extraction gap length of of 8 mm which is a setting for extracting the maximum current of hydrogen negative ions on the design was used in first deuterium operation in 2017 (Table 1). Typical extraction voltage between the PG and EG is 10 kV for the 170 kV acceleration voltage in hydrogen operation. Table 1 also shows summary of the $I_{acc(H)}$, the $I_{acc(D)}$, the $I_e/I_{acc(H)}$ and the $I_e/I_{acc(D)}$. The $I_{acc(D)}$ is lower than the The $I_{acc(H)}$ using the same accelerator in all beam lines in 2017. The current reduction rates are from 0.5 to 0.75. The ratios of $I_e/I_{acc(D)}$ increases in the deuterium operation, which are from 0.39 to 0.54.

A negative ion current and electron current are obtained by electrical current measurement in all NBI injectors, and also the optical emission intensity from cesium (Cs) neutral is observed by a wide range spectrometer. However, details of the plasma parameters in the vicinity of the PG surface in the injector source are not observed in LHD-NBI. Therefore, the difference of source parameters between hydrogen and deuterium is studied using the RNIS in the NBTS. In 2018 operation campaign, the extraction gap length is set 7 mm in BL3 in order increase the negative ion current after investigation of negative ion density and electron density in the RNIS in the test stand in NIFS. The $I_{acc(D)}$ increases to 55.4 A, and the $I_e/I_{acc(D)}$ could be suppressed to 0.31.

2.2. RNIS and diagnostic systems in NBTS

The RNIS is also equipped with a three-stage grid system with an arc discharge type negative ion source. The gird consists of two segments, and the GG uses slot type similar to the LHD-NBI. The beam width is the same as that of the LHD-NBI beam. Since the number of GG slots is 28 in RNIS, the scale factor compared with LHD-NBI is approximately 0.5. Although a hydrogen beam of 120 keV can be generated at the NBTS in NIFS, neutron generation using D^- beam acceleration is not permitted in the test stand, but the characteristics of arc discharge plasma using hydrogen and deuterium may be measured.

Various measurement devices are installed in the vicinity of the PG surface with the distance of 19 mm in the RNIS [23]. A negative ion density in both hydrogen and deuterium and an electron density is obtained by a Cavity-ring-down (CRD) method [24] and a millimeter wave interferometer (mmIF) [25], respectively. Since both density diagnostics are installed parallel to the PG surface in the minor axis direction of the arc chamber, measured densities are line averaged values. A plasma potential is obtained by a Langmuir probe (LP) [26,27]. Behavior of Cs neutral particles near the PG surface can be obtained by an optical emission spectroscopy (OES) [28,29] and a Cs laser absorption spectroscopy [23].

3. Change of Negative Ion Density and Electron Density by Gas Change Experiment

Before the deuterium operation, the negative ion source was operated by hydrogen for 3 months in LHD. The $I_{acc(H)}$ increase over 70 A in all injectors (see Table 1), and the total port through power of 15 MW was injected by 3 beam lines. The ratio of $I_e/I_{acc(H)}$ is 0.3 or less, and it is extremely favorable as 0.23 in BL3. At this time, the bias voltage was 3 V and the filling pressure was 0.3 Pa. In the hydrogen operation, since Cs is sufficiently coated on the surface of the PG, the Cs emission intensity did not change in 2-second beam operation even when Cs supply was stopped.

Figure 1 shows the shot history of the negative ion current (squares), the electron-ion current ratio (circles), and the optical emission signal from Cs neutral (diamonds) during the operation gas changing from H_2 to D_2 in the negative ion source in LHD-NBI. Deuterium gas is filled after evacuating the buffer tank and the feeder pipe of the gas supply unit. Replacement work has been done on site since the radiation level of LHD equipment has been reduced over the weekend. In order to adjust the arc discharge in the first deuterium operation, the supply of Cs was stopped after gas replacement. The source filling pressure was 0.3 Pa and the bias voltage is set to 3 V which is the same value in hydrogen operation.

Deuterium beam extraction is initiated using low arc discharge power ($P_{arc} \sim 50$ kW/source). The arc discharge power and the beam energy increase to 120 kW/source and 150 keV, respectively, until the shot number of 304242. The $I_{acc(D)}$ increases from 8

A to 35 A during this initial conditioning. Cs layer covering the PG surface is important for the production of negative ions. A Cs optical intensity (852.1 nm) normalized by the hydrogen/deuterium Balmer-γ intensity measured by OES in arc discharge phase, which is an index of the Cs neutral density near the PG surface [29], clearly increases after initiation of D$^-$ operation. The temperature of the PG is 230 °C in both H and D discharges. The higher Cs density in deuterium discharges compared to that in hydrogen discharges may be due to higher Cs sputtering by the heavier deuterium from the ion source walls and the plasma grid. The $I_e/I_{acc(D)}$ increases from 0.7 to 1 and then it immediately decreases to 0.5 by additional Cs feeding, which recovers the surface Cs-layer. Cs seeding is effective to increase the $I_{acc(D)}$ to 40 A. However, D$^-$ current did not recover to H$^-$ current level ($I_{acc(H)}$ = 70 A).

In order to investigate the reasons for the reduction of negative ion current and the increase of electron current in deuterium, the negative ion density and the electron density vicinity of the PG surface are investigated by the RNIS in the NBTS. Figure 2 shows the shot history of the negative ion density (n_{H-} for hydrogen and n_{D-} for deuterium: squares), electron density (n_e: circles), and the optical signal of Cs neutral normalized by Balmer-γ emission (diamonds) during the changing of the operation gas from H$_2$ to D$_2$. The gas replacement procedure is the same as LHD-NBI. Since the neutron production does not occur in the NBTS without beam extraction, deuterium discharge initiated immediately after gas replacement. In this situation, we can continuously supply Cs into the arc chamber with an oven temperature of 180 °C. The filling pressure and the bias voltage were set at 0.3 Pa and at 2.5 V, respectively, the same as hydrogen operation. The arc power is controlled to 50 kW, but it is temporarily reduced to 30 kW immediately after gas change, and then it recovers to 50 kW in a few shots. In the hydrogen phase, n_{H-} = 3.5×10^{17} m^{-3} is stably generated and n_e is also stable at 2×10^{17} m^{-3}, which is lower than n_{H-}. However in a deuterium discharge, n_{D-} is 4.6×10^{17} m^{-3}, which is 30% higher than the negative ion density in hydrogen, and n_e is 6.5×10^{17} m^{-3}, which is larger than n_{D-}, and >2.2 times higher than in the hydrogen discharge. Thus it seems that the increase of n_e/n_{D-} is mainly responsible for the increase in $I_e/I_{acc(D)}$. The need to maintain charge neutrality in the plasma in the vicinity of the PG means that the positive ion density must be increased in deuterium discharges compared to that in similar hydrogen discharges, i.e. an increase in n_{D-} is reflected in an increase in deuterium positive ion density. In the negative ion source of LHD-NBI, the extraction gap length and applied extraction voltage is not optimized for deuterium beam. Although the n_{D-} increases, the $I_{acc(D)}$ decreases because of the weak extraction field for deuterium negative ions. However, increasing the extraction field would probably cause an increase in the I_e, which is not desirable because of the consequent increase in the power to the extraction grid. Concern for this co-extracted electron is verified using a short extraction gap length in LHD-NBI in 2018, which will shown in section 5.

Another confirmation is about the state of Cs on the PG surface which is the production surface of negative ions. Intensity from Cs neutral particle also increases

for deuterium discharge. In order to verify the sputtering effect, we use a mixed gas discharge in the RNIS. The Cs neutral density in the vicinity of the PG is obtained by Cs laser absorption spectroscopy, as shown in Figure 3. Horizontal axis is the average mass number for mixture gas with helium with the percentages of 10%, 20%, and 30% in hydrogen, which are plotted between hydrogen and the deuterium atomic mass numbers. The Cs neutral particle density is 2.2×10^{14} m^{-3} in hydrogen discharge. That density increases to 6.5×10^{14} m^{-3} for deuterium discharge. This increasing rate is consistent with the increasing of Cs optical emission signal measured by the OES. We also confirmed the increase of Cs density for hydrogen and He mixed plasma, which depended on the He fraction. Therefore, the Cs layer on the PG and the walls of the ion source is depleted by increased sputtering by deuterium compared to that with hydrogen because of the higher mass of deuterium. Maintaining the Cs layer on the PG in order to maintain the required negative ion production rate is one of the issues with operation in deuterium.

4. Effect of Electron Suppression by Bias Voltage

In the negative ion source of LHD-NBI, a magnetic filter is used for suppressing the inflow of electrons from the arc discharge region to the extraction region vicinity of the PG. However, the magnetic filter field is created by permanent magnets, and they are not easily changed. Therefore the bias voltage (V_{bias}) applied between the ion source and the PG is used.

Figure 4(a) shows the change of the $I_{acc(H)}$ and the I_e for the V_{bias} in the hydrogen operation in LHD-NBI. We normally use 2 - 3 V low bias voltage, which depends on the value of $I_{acc(H)}$ and $I_e/I_{acc(H)}$. The bias voltage suppresses not only electrons but also negative ions, see Figures 4. Therefore, higher V_{bias} is not an advantage for high power beam generation. In hydrogen discharge, a small increase in I_e is observed even with a low V_{bias}. However, $I_e/I_{acc(H)}$ is 0.3 when the V_{bias} is 2 V. Figure 4(b) shows the dependence of the n_{H^-}, the n_e, and the plasma potential (ϕ) measured by the CRD, the mmIF, and the LP, respectively, on the V_{bias} in the RNIS. In the case of the 3 V bias voltage, the n_{H^-} and the n_e are 3×10^{17} m^{-3} and 0.7×10^{17} m^{-3}, respectively. The density ratio of $n_e/n_{H^-} = 0.23$ is consistent with $I_e/I_{acc(H)}$ in LHD-NBI. The n_{H^-} and the n_e each decrease as V_{bias} increased. The ϕ increases from 1 V to 4V by increasing the V_{bias} (0 - 8 V). Quasi neutrality in the plasma means that the decrease in the n_{H^-} and the n_e that accompany the increase in the positive potential of the PG must be accompanied by a decrease in the H$^+$ density. It is considered that the influx of electrons maintaining the charge neutrality also decreases in the extraction region at high bias voltage.

On the other hand, an increase in n_e is clearly observed in the deuterium operation of the RNIS. Figure 5(a) shows the change of the $I_{acc(D)}$ and the I_e for the V_{bias} in the deuterium discharge of the LHD-NBI. The $I_{acc(D)}$ is saturated, and the electron current increases greatly at the V_{bias} lower than 5 V. The $I_e/I_{acc(D)}$ is 0.7 with the low V_{bias} of

2 V, which is not a permissible value for safety beam operation to prevent damage to the EG surface due to electron current. Therefore, the V_{bias} in the range of 5 - 6 V is the standard setting for deuterium beam operation in LHD-NBI. Figure 5(b) shows the dependence of the n_{D^-}, n_e, and ϕ on the V_{bias} for deuterium discharge in the RNIS. The plasma potential of deuterium discharge is same as that in hydrogen discharge (1 - 4V). The n_e is larger than the n_{D^-} in the lower bias setting ($V_{bias} < 2.5$V). These densities are the same value (5×10^{17} m^{-3}) at the $V_{bias} = 2.5$ V, and the n_e and the n_{D^-} are 5 times and 1.6 times higher than the n_e and the n_{H^-} in hydrogen discharge, respectively. The n_e decreases to 2.5×10^{17} m^{-3} at the $V_{bias} = 5.6$ V, which is sufficiently lower than the n_{D^-} (4×10^{17} m^{-3}) in the vicinity of the PG surface. If the n_{H^-} and n_{D^-} are the same in the vicinity of PG aperture, the maximum deuterium negative ion current should be limited to $1/\sqrt{2}$ times the hydrogen negative ion current by Child-Langmuir law using the same extraction gap length with the same extraction voltage. Therefore, the $I_{acc(D)}$ of 46 A in deuterium operation using 5.6V bias voltage is consistent with the the product of the reduction rate (0.7) and the $I_{acc(H)}$ of 70 A in hydrogen using the same arc discharge power (170 kW/source) in LHD-NBI. The density ratio of n_e/n_{D^-} is 0.6 in RNIS, which is also comparable value with the $I_e/I_{acc(D)}$ (0.2 - 0.6 shown in section 5) in LHD NBI. Therefore, the ratio of $I_e/I_{acc(D)}$ is closely related to the ratio of n_e/n_{D^-} in the vicinity of the PG. If the electron density in the vicinity of the PG can be maintained sufficiently lower than the negative ion density by the bias voltage, co-extracted electrons can be reduced. Under this conditions, it is expected that a strong extraction electric field can increase the negative ion current while maintaining a low co-extracted electron. For that reason, we test a short gap length to extract deuterium negative ion beam in 2018 experimental campaign.

5. Influence of Co-extracted Electron by Arc Discharge Power

The thermal load of the beam accelerator caused by co-extracted electrons is an issue in high power and long pulse beam operation in N-NBI. The extracted electrons are bent by the electron deflection magnetic (EDM) field installed in the EG [5], and electrons are absorbed by the EG. Although the EG is cooled by a water flow, concentration of electrons causes damage to the EG surface in high power beam operation. For this reason, the influence of arc discharge power on negative ions and co-extracted electrons in the beam is investigated.

Figure 6 (a) shows the dependence of the $I_{acc(H)}$ and $I_{acc(D)}$ by two ion sources on the arc discharge power (P_{arc}) in LHD-NBI. Since two negative ion beams are accelerated by one high voltage power supply in LHD-NBI, these current are the sum of two acceleration currents from the negative ion sources. The horizontal axis is the total P_{arc} by two ion sources in Figures 6. Circle marks are the $I_{acc(H)}$ and square marks are the $I_{acc(D)}$ in 2017. The negative ion current linearly increases with respect to the P_{arc} and is not saturated. The averaged value of the ratio of $I_{acc(D)}/I_{acc(H)}$ is approximately 0.66 for the same arc discharge power. Star mark is the $I_{acc(D)}$ using short extraction gap length

(PG - EG : 7mm) in 2018. The bias voltage and filling pressure is set 5.6V and 0.43 Pa, respectively, these are the same as the settings in 2017. The $I_{acc(D)}$ of 55.4 A with the averaged current density of 223 A/m^{-3} is generated by two ion sources (Table 1). We can use high P_{arc} of 400kW (i.e. 200 kW/source) in the deuterium operation, which is same as the P_{arc} in hydrogen operation. The reason for increasing the P_{arc} is reduction of the $I_e/I_{acc(D)}$ in deuterium operation.

We also continue maintaining the low I_e in deuterium as large as that in hydrogen beam using conservative bias and pressure setting, which contributes to safety beam operation in the first deuterium campaign in LHD. A strong dependence of $I_e/I_{acc(D)}$ on the P_{arc} appeared in the deuterium beam operation, as shown in Figure 6(b). In the case of hydrogen operation, the $I_e/I_{acc(H)}$ distribute between 0.2 and 0.3. The lower limit of $I_e/I_{acc(H)}$ slightly increases as increasing P_{arc}, which corresponds to the optimum operation in which electrons are suppressed with the maximum beam current. In deuterium discharge, $I_e/I_{acc(D)}$ are widely distributed (0.2 - 0.6) which including the adjusted phase data using lower P_{arc} (100 - 150 kW/source) while investigating the dependency of V_{bias} and filling pressure. The lower limits of $I_e/I_{acc(D)}$ are 0.2 in both hydrogen and deuterium discharges in 100 kW/source. However, the $I_e/I_{acc(D)}$ increases greatly with the increase of the arc power, which is the unique characteristic in deuterium operation. The $I_e/I_{acc(D)}$ increases to 0.39 at the P_{arc}= 170 kW/source in high $I_{acc(D)}$ operation, which is twice larger than the $I_e/I_{acc(H)}$ in hydrogen operation using same P_{arc}. The thermal load on the EG due to co-extracted electron is in a safety level in the operations near the lower limit of $I_e/I_{acc(D)}$ in this operation. However, the gradient of the slope is 6.4 times higher than that of hydrogen, thus if the ion source will be operated using higher arc discharge power, the thermal load due to electrons will become a problem. Thus, this trend is an important issue for considering the production of high-power deuterium beam in every N-NBI. Star mark is the result of $I_e/I_{acc(D)}$ using short gap length (7 mm) in 2018. The $I_e/I_{acc(D)}$ decreases to 0.31 in the P_{arc} of 200 kW/source with the 5.6 V bias voltage and the 0.43 Pa filling pressure. The $I_e/I_{acc(D)}$ using short gap length is much lower than the lower limit value of $I_e/I_{acc(D)}$ in 2017, which is almost equal to the $I_e/I_{acc(H)}$ in hydrogen operation. Since the $I_e/I_{acc(D)}$ ratio can be maintain low, high arc power operation for increasing the $I_{acc(D)}$ current become possible.

Figure 7 shows changes in negative ion density and electron density for arc discharge power in the RNIS. The negative ion densities increase as the arc power increases, and the n_{D^-} is higher than the n_{H^-}. It is considered that the ionization and the dissociation in the discharge region increase, and neutral particles and positive ions which are the sources of negative ions, increase. Since the mass of deuterium is heavier than hydrogen, the diffusion coefficient is lower and the confinement of deuterium in the vicinity of the PG should be improved. On the other hand, the electron density also increases as the arc power increases, but that density differs greatly between hydrogen discharge and deuterium discharge. The electron density in deuterium discharge is 4 times larger than the electron density in hydrogen discharge. The density fraction of n_e/n_{H^-} is as low

as 0.17 in 60 kW discharge power, but the n_e/n_{D^-} is 0.61. Although the result of the n_e/n_{D^-} is slightly larger than the $I_e/I_{acc(D)}$ ratio range shown in Figure 6(b), there is the common tendency of electron increasing. Therefore, an increase in electron density due to a high arc power is considered to be responsible for an increase in the $I_e/I_{acc(D)}$ in deuterium discharge.

Here, we must discuss a distribution of negative ion density and electron density perpendicular to the PG surface to understand electron contamination in the beam. We obtained flow direction of negative hydrogen ion during beam extraction by laser assisted directional Langmuir probe in RNIS [26,30]. According to the result, the turning point of negative hydrogen ion which released from the PG surface return to the PG direction was approximately 20 mm from the PG. This was also confirmed by the two-dimensional distribution of the extraction of negative hydrogen ion measured by the H_α imaging diagnostic [31, 32]. The extraction distribution of hydrogen negative ions was strongly distributed near the PG aperture in the range of $0 < z < 20$ mm, here z is the distance from the PG surface, which is closely related to the distribution of EDM field in the vicinity of PG surface. A negative ion rich plasma with low electron is formed in the region between PG and EDM lobe [23, 30]. The negative ion density should decrease outside the turning point of negative ions, and it is considered that the inflow of electrons from the discharge region increases. In the case of deuterium discharge, the velocity of the D^- ions generated from the PG should be 0.7 times of H^- velocity if both ions have the same energy. If the turning point of the deuterium negative ion is closer to the PG, then the area with high electron density should be closer to the PG. The reduction in the electron density and control of its distribution in the vicinity of the PG is one of the key parameters to reduce the co-extracted electrons current.

On the other hand, the response of the n_{H^-}, the n_{D^-} and the n_e to the V_{bias} to suppress co-extracted electrons is very interesting. It is well known that electron current extracted from a volume-production negative ion source increases with deuterium discharge [33]. Since the decay curve of the electron current for bias voltage was shifted by about 2 V, it was presumed that the change was due to the difference in the plasma potential. However, in the surface-production negative ion source of the RNIS, there is no difference in plasma potential between hydrogen and deuterium discharge. As the bias voltage decreases, the plasma potential decreases. However the electron density and the negative ion density increase in lower plasma potential. Since the sum of the electron density and the negative ion density is strongly related to the positive ion density by the charge neutrality, the D^+ ion density in the deuterium discharge is larger than the H^+ ion density in the same bias condition. Increase of D^+ ions is because the decrease of D^+ ion velocity owing to weight of the D^+ is twice as heavy. In the surface-production negative ion source, most of the negative ions in the vicinity of the PG are supplied from the PG surface, so that electrons accompanying the positive ions from the discharge region bridge the gap between the negative ion density and the positive ion density by charge neutrality. By suppressing positive ion density at high bias voltage, electrons entering along with positive ions are also suppressed. Therefore, it is considered that control of

positive ions in the vicinity of the PG is also important factor to suppress co-extracted electrons.

6. Conclusion

Deuterium negative ion beam operation for LHD-NBIs was initiated in 2017. The $I_{acc(D)}$ of 46 A has been extracted for 2 sec with the averaged current density of 190 A/m^2 by two negative ion sources in the injector in first deuterium campaign. The ratio of $I_e/I_{acc(D)}$ was 0.39. Although the configuration of the ion source was not optimized for deuterium, the observed $I_{acc(D)}$ reached 82% of the LHD requirement in the first phase deuterium beam operation, and those results were comparable to the ITER-NBI specification (40 A negative ion current with the current density of 200 A/m^2 at 0.3 Pa). Linear dependence of the minimum value of the $I_e/I_{acc(D)}$ on the P_{arc} was found, and was stronger than the $I_e/I_{acc(H)}$, which is one of the issue for deuterium operation. A clear increase in electron density in the vicinity of the PG was confirmed by the RNIS. Changes in electron density and negative ion density at the switching of operation gas from hydrogen to deuterium in the RNIS agree with the trend of beam current in the LHD-NBI. A bias voltage satisfying the condition of $n_{D^-} > n_e$ in the vicinity of the PG realizes a high $I_{acc(D)}$ and a low I_e using a strong extraction field between the PG and the EG. The $I_{acc(D)}$ current of 55.4 A (averaged current density : 233 A/m^2 is achieved for 1.5 sec using the short gap length (7 mm) in 2018. The lower $I_e/I_{acc(D)}$ of 0.31 is maintained by 200 kW/source high-discharge power operation, which becomes the same level as the $I_e/I_{acc(H)}$ in hydrogen operation.

Acknowledgments

References

[1] M. Kuriyama *et al* , Fusion Tech. 1996 (Proc. 19th Symp. Fusion Tech. Lisbon, 16-20 Sep. 1996) (1996) 693 - 696.
[2] A. Kojima *et al* , Nucl. Fusion **51**, (2011) 083049.
[3] A. Iiyoshi *et al* , Nucl. Fusion **39**, (1999) 1245.
[4] O. Kaneko *et al* , Nucl. Fusion **43**, (2003) 692.
[5] Y. Takeiri *et al* , Rev. Sci. Instrum. **71**, (2000) 1225.
[6] K. Tsumori *et al* , Rev. Sci. Instrum. **75**, (2004) 1847.
[7] T. Mutoh *et al* , Fusion Science and Technology **68**, (2015) 216 - 224.
[8] K Tsumori *et al* , Plasma Sci. Technol. **8** (2006) 24.
[9] R. Hemsworth, A. Tanga and V. Antoni, Rev. Sci. Instrum. **79**, (2008) 02C109.
[10] M. J. Singh *et al* , New J. Phys. **19**, (2017) 055004.
[11] P. Sonato *et al* , Fusion Eng. Des. **84**, (2009) 269 - 274.
[12] V. Toigo *et al* , New J. Phys. **19**, (2017) 085004.
[13] W. Kraus *et al* , Rev. Sci. Instrum. **89**, (2018) 052102.

[14] K. Ikeda *et al* , AIP Conference Proceedings **2011**, (2018) 060002.

[15] Y. Takeiri *et al* , Rev. Sci. Instrum. **68**, (1997) 2003.

[16] Y. Takeiri *et al* , Fusion Sci. Technology **58**, (2010) 482 - 488.

[17] M. Osakabe *et al* , IEEE Transactions on Plasma Science **46**, (2018) 2324 - 2331.

[18] M. Osakabe, *et al* , Fusion Sci. Technology, **72**, (2017)199 - 210.

[19] M. Kobayashi, *et al* , Fusion Eng. Des., **137**, (2018) 191-195.

[20] Y. Takeiri *et al* , Nucl. Fusion **46**, (2006) S199 - S210.

[21] M. Kisaki *et al* , Rev. Sci. Instrum. **87**, (2016) 02B321.

[22] K. Tsumori *et al* , Plasma Sci. Technol. **8** (2006) 24.

[23] K. Tsumori and M. Wada, New J. Phys. **19**, (2017) 045002.

[24] H. Nakano *et al* , AIP Conference Proceedings **1390**, (2011) 359.

[25] T. Tokuzawa *et al* , Rev. Sci. Instrum. **87**, (2016) 11E105.

[26] S. Geng *et al* , Rev. Sci. Instrum. **87**, (2016) 02B103.

[27] K. Tsumori *et al* , AIP Conference Proceedings **1869**, (2017) 030001.

[28] K. Ikeda *et al* , AIP Conference Proceedings **1390**, (2011) 367.

[29] K. Ikeda *et al* , AIP Conference Proceedings **1869**, (2017) 050004.

[30] S. Geng *et al* , Fusion Eng. Des. **123**, (2017) 481 - 484.

[31] K. Ikeda *et al* , New J. Phys. **15**, (2013) 103026.

[32] K. Ikeda *et al* , AIP Conference Proceedings **1655**, (2015) 040005.

[33] T. Inoue *et al* , Rev. Sci. Instrum. **61**, (1990) 496-498.

Table 1. Setting of extraction gap length and the results of the negative ion current and the electron-ion current ratio in in LHD-NBI

Year	Beam line	Ext. gap	GG type	$I_{acc(H)}$	$I_e/I_{acc(H)}$	$I_{acc(D)}$	$I_e/I_{acc(D)}$
2017	BL1	7 mm	Slot	81.5 A	0.27	41.6A	0.49
2017	BL2	8 mm	Aperture	74.2 A	0.30	45.5A	0.54
2017	BL3	8 mm	Slot	77.5 A	0.23	46.2 A	0.39
2018	BL3	7 mm	Slot	73.9 A	0.25	55.4 A	0.31
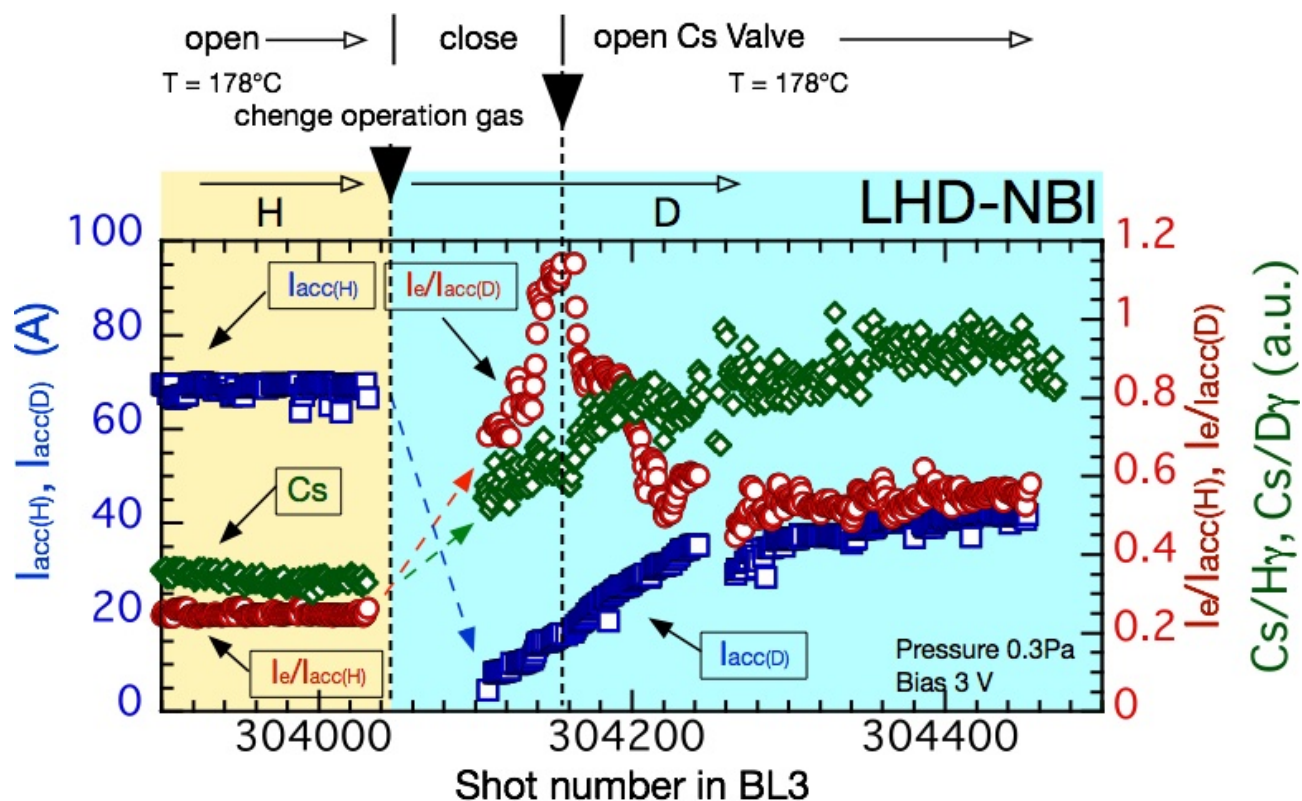
Figure 1. Shot history of the $I_{acc(H)}$ and $I_{acc(D)}$ (squares), $I_e/I_{acc(H)}$ and $I_e/I_{acc(D)}$ (circles), and the optical signal of Cs neutral (diamonds) during the operation gas changing from H_2 to D_2 in the negative ion source. The P_{arc} is 160 kW/source in hydrogen discharge. Deuterium beam operation initiated $P_{arc} = 50$ kW and increased to 120 kW/source. Deuterium negative ion current decreased to 60% of hydrogen ion current in the first trial. The $I_e/I_{acc(D)}$ largely increased by deuterium discharge, but it recovered by additional Cs feeding. Reproduced from Figure 2 in AIP Conference Proceedings 2011, 060002 (2018); `https://doi.org/10.1063/1.5053331`, with the permission of AIP Publishing.
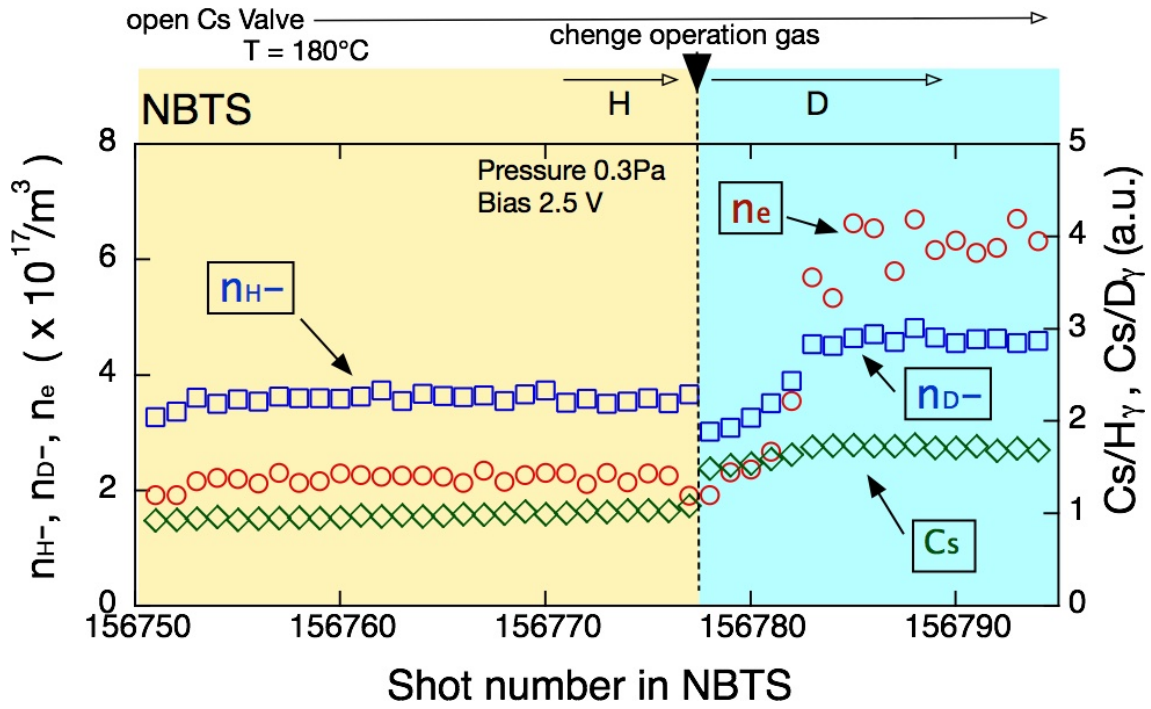
Figure 2. Shot history of the n_{H^-} and n_{D^-} (squares), n_e (circles), and the optical signal of Cs neutral (diamonds) in the vicinity of PG surface during the operation gas changing from H_2 to D_2 in the RNIS. The P_{arc} is 50 kW in hydrogen and deuterium discharge, which is temporarily reduced to 30 kW in a few shots immediately after gas change.
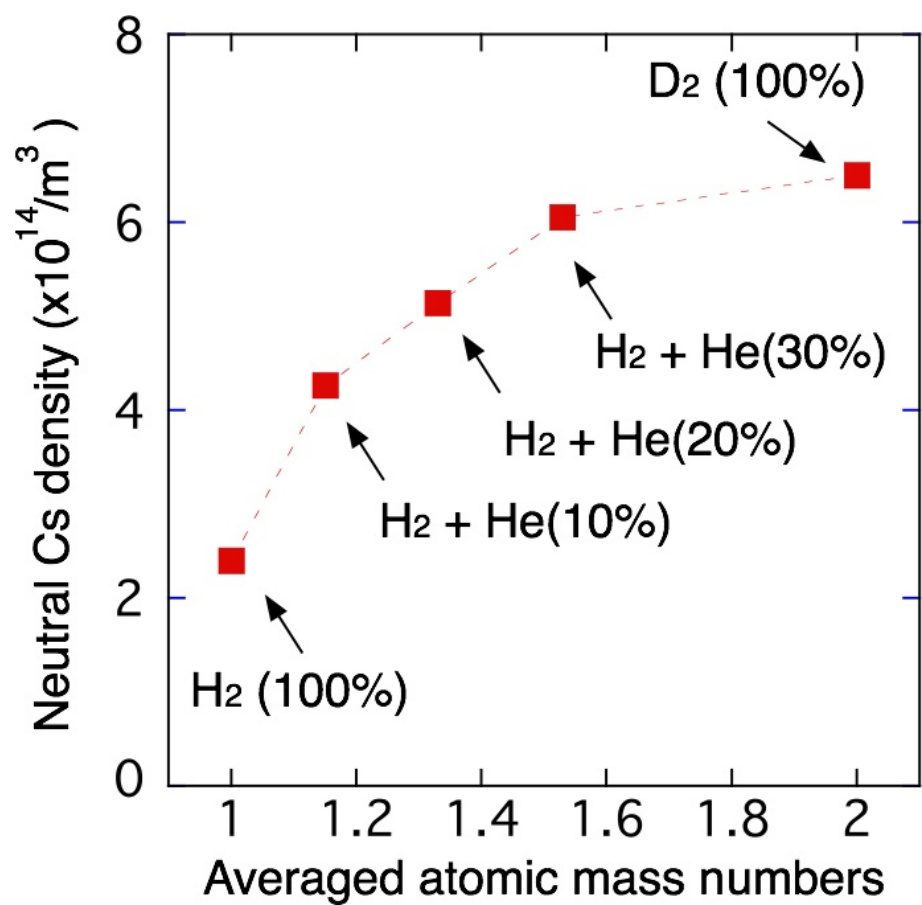
Figure 3. Neutral Cs density measured by the Cs laser absorption diagnostic for hydrogen, deuterium, and helium mixed hydrogen discharge with low discharge power of $P_{arc} = 28$ kW in the RNIS.
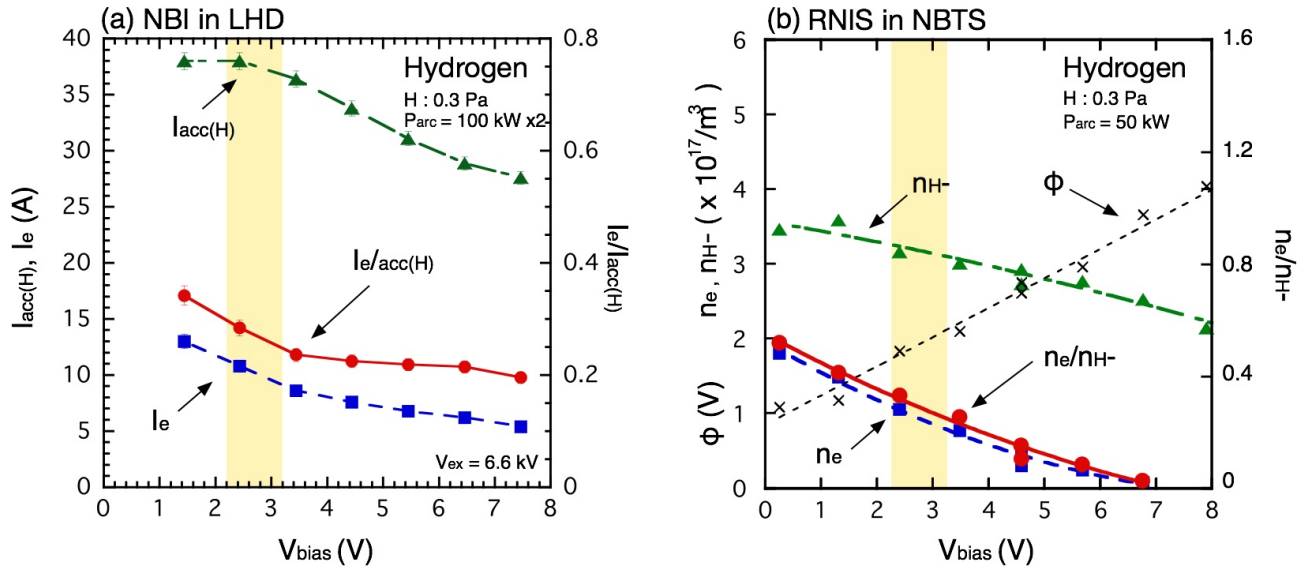
Figure 4. (a) Dependence of the $I_{acc(H)}$ (triangle), the I_e (square), and the $I_e/I_{acc(H)}$ (circle) in LHD-NBI on the bias voltage. Reproduced from Figure 3 in AIP Conference Proceedings 2011, 060002 (2018); `https://doi.org/10.1063/1.5053331`, with the permission of AIP Publishing. (b) Dependence of the n_{H^-} (triangle), the n_e (square), the n_e/n_{H^-} (circle), and the plasma potential ϕ (cross) at 19 mm from the PG in the RNIS in the NBTS on the bias voltage. Shaded area is the range of the V_{bias} setting that is normally used for the hydrogen operation in LHD-NBI.
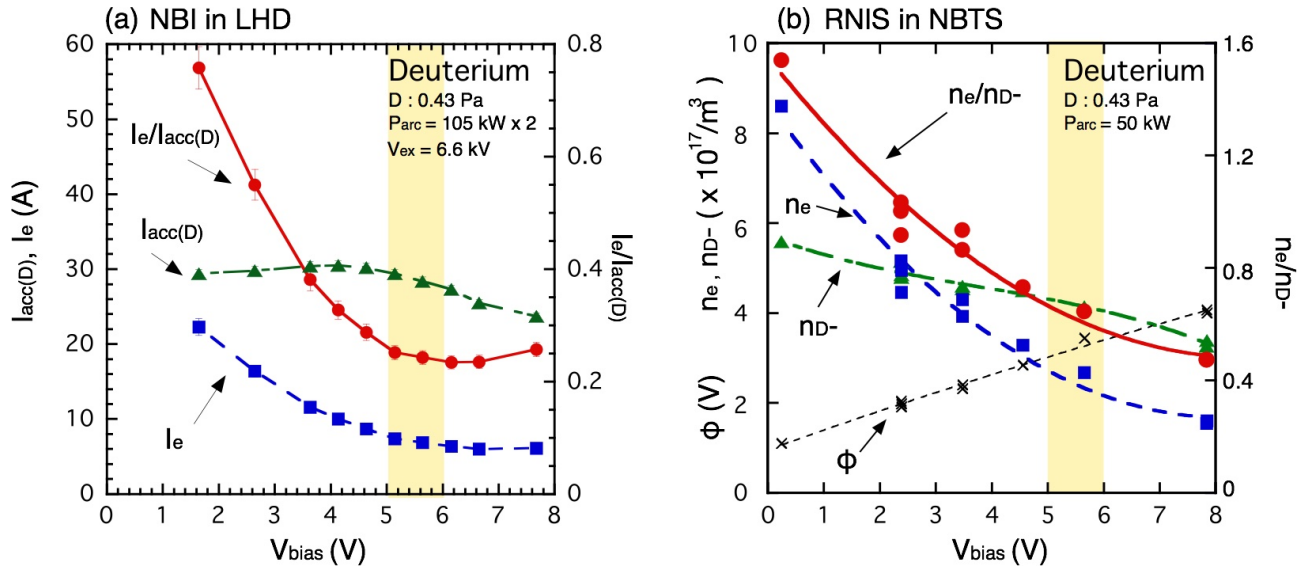
Figure 5. (a) Dependence of the $I_{acc(D)}$ (triangle), the I_e (square), and the $I_e/I_{acc(D)}$ (circle) in LHD-NBI on the bias voltage. Reproduced from Figure 3 in AIP Conference Proceedings 2011, 060002 (2018); `https://doi.org/10.1063/1.5053331`, with the permission of AIP Publishing. (b) Dependence of the n_{D^-} (triangle), the n_e (square), the n_e/n_{D^-} (circle), and the ϕ (cross) at 19 mm from the PG in the RNIS in the NBTS on the bias voltage. Shaded area is the range of the V_{bias} setting that is normally used for the deuterium operation in LHD-NBI.
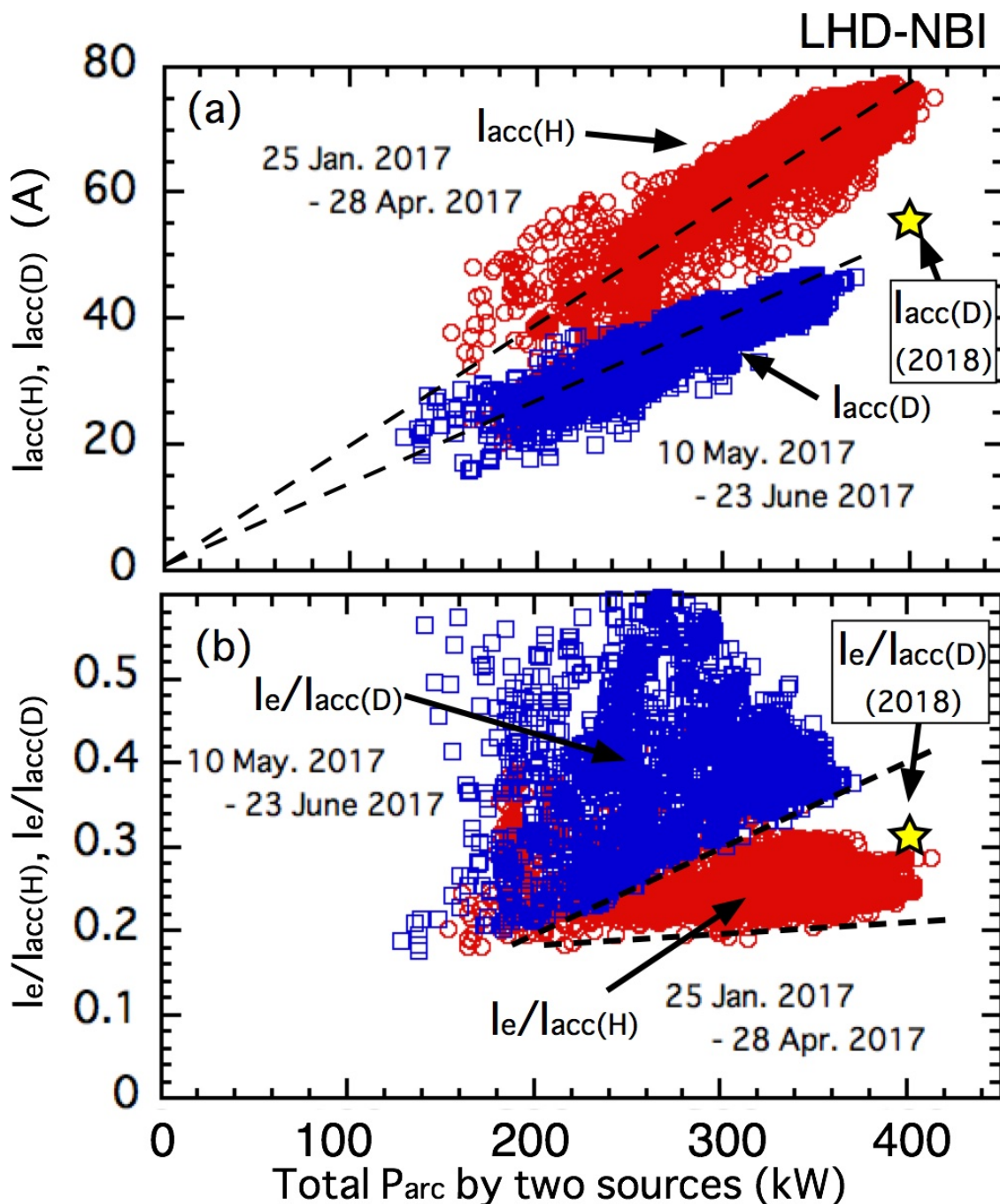
Figure 6. Dependence of (a) the $I_{acc(H)}$ and the $I_{acc(D)}$, (b) the $I_e/I_{acc(H)}$ and the $I_e/I_{acc(D)}$ on the total P_{arc} by 2 ion sources for hydrogen discharge (circle) and deuterium discharge(square) using 8 mm extraction gap length optimized for H⁻ operation in LHD-NBI in 2017. Star marks are the results of D⁻ operation using short gap length (7 mm) in 2018. Reproduced from Figure 4 in AIP Conference Proceedings 2011, 060002 (2018); `https://doi.org/10.1063/1.5053331`, with the permission of AIP Publishing.
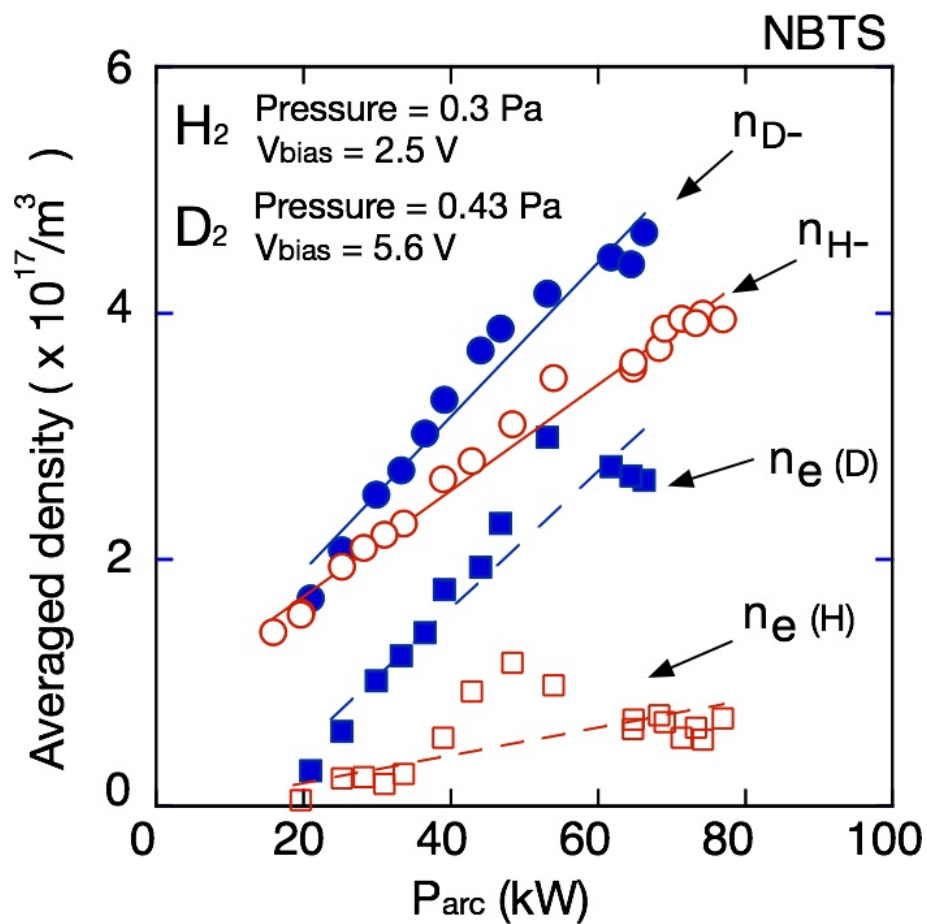
Figure 7. Dependence of the negative ion density (circle) and electron density (square) for hydrogen discharge (open) and deuterium discharge (closed) in the RNIS in the NBTS on the arc discharge power.